E-band full corporate-feed 32 × 32 slot array antenna with simplified assembly

Zhao, Hui; Lu, Yunlong; You, Yang; You, Qingchun; Wang, Yi; Yang, Wen-wen; Huang, Jifu

DOI:
10.1109/LAWP.2021.3055763

E-band Full Corporate-Feed 32 × 32 Slot Array Antenna with Simplified Assembly

Hui Zhao, Yunlong Lu, Yang You, Qingchun You, Yi Wang, *Senior Member, IEEE,* Wen-Wen Yang, *Member, IEEE,* and Jifu Huang

***Abstract*—This letter presents a high-gain 32 × 32-element full corporate-feed array antenna using a simplified assembly of only two split blocks. This is made possible by a new feeding configuration which eliminates the cavity-backed layer used in conventional designs. E-plane T-junctions, as well as the single-ridge waveguide output structure, are used in the full corporate-feed network to reduce its size. This helps to realize the one-to-one corresponding excitation between the output port of the feed network and the radiation slots. In addition, a transition structure from single-ridge waveguide to double-ridge waveguide is employed to improve the impedance matching bandwidth of the radiation part. For demonstration, a prototype is designed, fabricated and measured. Experimental results show that the array antenna achieves an impedance bandwidth of 19% (71-86 GHz) with input reflection coefficient better than −13 dB, the antenna efficiency of over 76.4%, and peak gain of better than 38.4 dBi over the entire operating band.**

***Index Terms*—Slot arrays, millimeter-wave arrays, double-block structure, full corporate-feed network.**

I. Introduction

THE frequency range of 71–76 and 81–86 GHz in E-band has been allocated for high-data rate communication, such as millimeter-wave (mmW) point-to-point links [1]. Low profile wideband and high-gain planar array antennas are highly desired in such fixed radio links. Hollow-waveguide slot array antenna is advantageous over microstrip feed array antennas [2-4] for a large-size high gain array, since hollow waveguide does not suffer from dielectric or radiation losses.

According to the structures of feed network, hollow-waveguide based mmW slot array antennas can be divided into two categories: one is series-feed [5], [6] or partial cooperate-feed [7], [8] and the other is full corporate-feed [9-11]. The former generally has a simpler structure, but usually suffers from narrow bandwidth [12-14]. In contrast, the full corporate-feed array antenna exhibits a wider bandwidth. MmW full corporate-feed slot array antennas have been reported in [9-11], [15-21]. In [17], a W-band slot array antenna with fractional bandwidth (FBW) of 21% (85 - 105 GHz) and a peak gain of over 30 dBi was presented. An E-band hollow-waveguide full cooperate-feed 32×32-slot array antenna using polyetherimide fabrication was introduced in [18]. The operating band covers from 71 to 86 GHz with a peak gain of over 37 dBi. The mmW full corporate-feed slot arrays in [19-21] were implemented using diffusion bonding technology. However, these antennas required at least three split functional blocks in fabrication to the form the structure: the feeding block, the coupling block (or cavity backing) and the radiation block. It is highly desirable and beneficial if the number of required fabrication blocks can be reduced, because the manufacture cost increases with the blocks so does the risk of electromagnetic energy leakage from imperfect contacts between the blocks.

This work sets to design an E-band full corporate-feed array using minimum number of fabrication blocks based on hollow waveguide. A double-block structure with the radiation block and the feed network only is proposed and realized, by eliminating the coupling layer in conventional designs. This allows a two-part split-block structure, which significantly eases the fabrication and assembly. However, this leads to the challenge of realizing one-to-one excitation between the output ports of the feed network and the radiation slots. A solution is devised and demonstrated in a 1-to-1024 (32 × 32) power divider: E-plane T-junctions are used to construct the power divider with all the output ports converted to single-ridge waveguides for reducing the port size. For validation, a prototype operating at 71–86 GHz is fabricated and measured.

II. Antenna Configuration and Analysis

Fig. 1(a) shows the configuration of the 32 × 32-slot array antenna. It consists of only two functional blocks: the radiation block M1, and the feed block M2. This is different from the feed-coupling-radiation configurations used in [19-21]. The radiation block, to be machined in one piece, contains the radiation slots and the transition structures from single-ridge waveguide to double-ridge waveguide. The 1-to-1024 (32 × 32) power divider is used to excite the radiation slots directly. The feed block is constructed of multiple H-shape power dividers with single-ridge waveguide output structure and it is machined in one piece. The aluminum-magnesium alloy with a finite conductivity of 3.1×10^7 S/m is used in this design. The detailed analysis of these two blocks will be discussed in following

This work was supported partly by National Key R&D Program of China under Project 2018YFB1802100, in part by National Natural Science Foundation of China under Projects 61801252, 61631012, and U1809203, in part by Zhejiang Natural Science Foundation under Project LY21F010002, Ningbo Natural Science Foundation under Project 202003N4108 and the Fundamental Research Funds for the Provincial Universities of Zhejiang under grant no. SJLY2020001, in part by K.C. Wong Magna Fund in Ningbo University. Yi Wang was supported by the U.K. Engineering and Physical Science Research Council under Contract EP/S013113/1.

Hui Zhao, Yunlong Lu, Yang You, Qingchun You, and Jifu Huang are with the Faculty of Electrical Engineering and Computer Science, Ningbo University, Ningbo 315211, China (e-mail: luyunlong@nbu.edu.cn).

Yi Wang is with the School of Engineering, University of Birmingham, Birmingham B15 2TT, U.K. (e-mail: y.wang.1@bham.ac.uk).

Wen-Wen Yang is with the School of Information Science and Technology, Nantong University, Nantong 226019, China (e-mail: wwyang2008@hotmail.com).

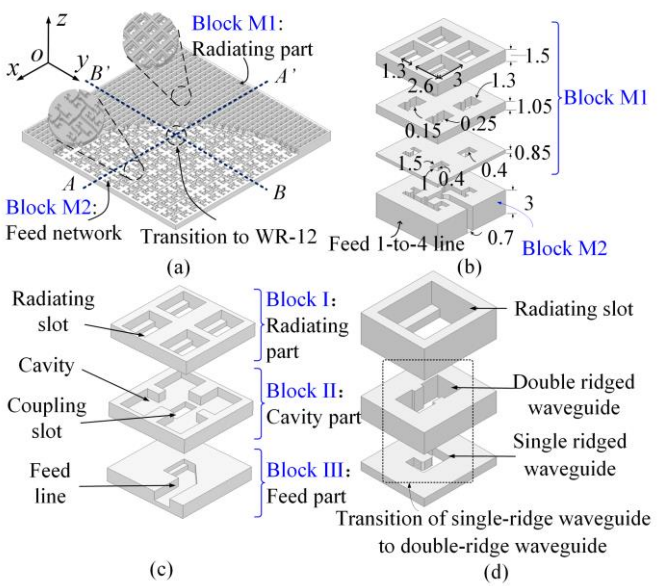

Fig. 1. (a) Configuration of the proposed array antenna. (b) Detailed three-dimensional (3-D) view of a 2 × 2 slot sub-array, (c) Detailed 3-D view of a conventional 2 × 2 slot sub-array [19-21], (d) Detailed 3-D view of a single channel of the radiation layer (Block M1) in the proposed array. All dimensions are given in millimeters.

sections. All simulations are performed using Ansoft HFSS, and the metal surface roughness of 0.5 μm is included in the simulation.

A. Radiation block

To facilitate comparison with previous work, we designate a 2×2-slot to be the sub-array as shown in Fig. 1(b) together with the optimized dimension values. It should be noted that the top three layers shown in Fig. 1(b) are actually sliced from a single block (the radiation block). Unlike the conventional sub-arrays in previous work [19-21], the 1-to-4 cavity backing to the slots (the Block II shown in Fig. 1(c)) is eliminated in this design. Instead, each output terminal in the feed block feeds one radiation slot through a ridge waveguide transition. This means the number of output ports of the power divider in the feed network should be the same as the number of radiation slots, which increases the layout and design difficulty of the feed network (to be discussed in Section II-B).

Fig. 1(d) further shows the waveguide transition structure to the slot in block M1. The flared radiation slot improves the impedance matching bandwidth between the radiation slot and free space. The periods of the radiation slots in *x*- and *y*-directions are both selected to be a wavelength in free space at the maximum operating frequency. The transition from the single-ridge waveguide to double-ridge waveguide helps achieve wideband impedance matching between the feed-network and the slot. The comparisons of reflection coefficient with or without the double-ridged waveguide structure is plotted in Fig. 2(a). Without the double-ridge waveguide structure, the single-ridge waveguide cannot directly match the radiation slot due to the large difference in characteristic impedance. The double-ridge waveguide structure functions as an impedance transformer, which helps to achieve a wideband impedance matching over the frequency range of 69.5 - 86.5 GHz with $|S_{11}|$<-20 dB. The radiation patterns of the 2×2 sub-

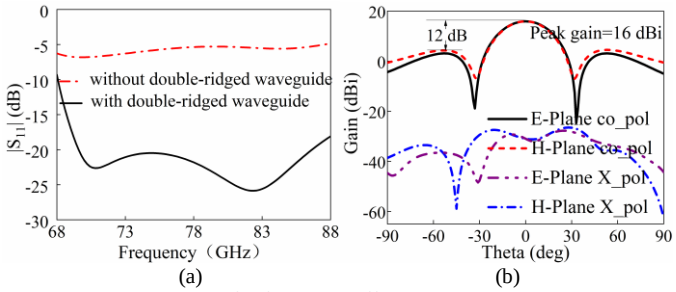

Fig. 2. (a) Comparisons of reflection coefficient with or without the double-ridged waveguide structure; (b) Simulated radiation patterns of the sub-array at 78.5 GHz.

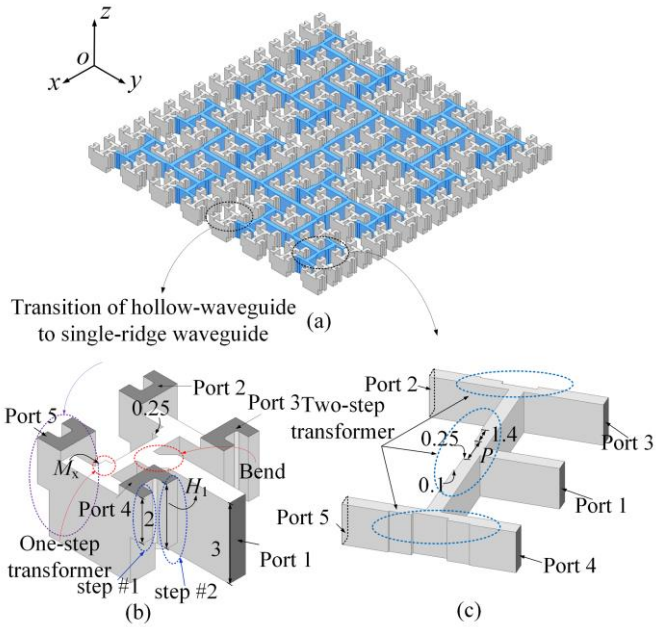

Fig. 3. (a) Quarter of full corporate-feed network. (b)Type-I and (c) Type-II H-shape power dividers. All dimensions are given in millimeters.

array at the center frequency of 78.5 GHz is plotted in Fig. 2(b). It can be seen that the peak gain is 16 dBi with the sidelobe suppressed by more than 12 dB and cross-polarization of less than -40 dB in both *E*- and *H*-planes.

B. Feed block

As pointed out previously, the radiation slots in block M1 and the output ports of feed network in block M2 have a one-to-one correspondence. As a result, the distance between the adjacent output ports in the feed should be the same as the period of radiation slots. Considering the symmetry of the array antenna (see the symmetry lines A-A' and B-B' in Fig. 1(a)), only a quarter of the full corporate-feed network is shown in Fig. 3(a). It is based on multiple cascaded H-shape 1-to-4 power dividers. The input port of the feed network is a standard WR-12 waveguide at the center of back side. Two types of H-shape power dividers are used, namely Type-I and Type-II shown in Fig. 3(b) and (c) respectively. Type-I is used as the final stage of the feed network whereas other H-shape power dividers adopt Type-II structure. In order to reduce cross sectional area of the whole feed network, E-plane T-junctions are employed. In addition, the single-ridge waveguide at the outputs of Type-I divider is used to further reduce the size of output ports. A bent structure is used at the input part of the Type-I power

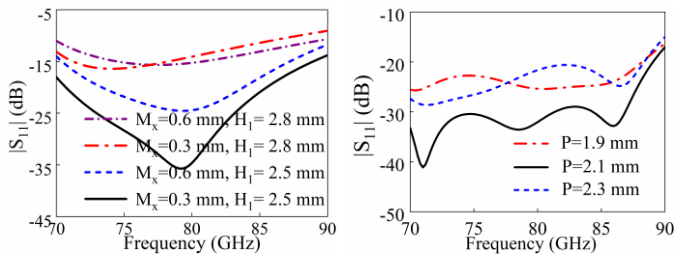

(a) (b)

Fig. 4. Simulated reflection coefficient with (a) different values of *Mx* and H_1; and (b) different values of *P*.

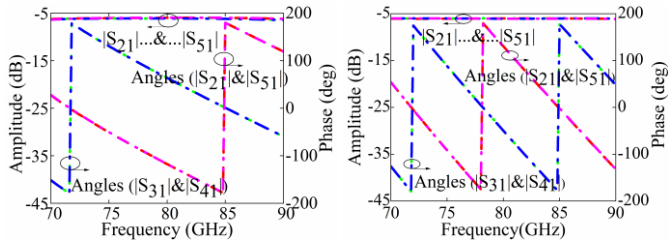

(a) (b)

Fig. 5. Amplitude and phase of (a) Type-I H-shape power divider. (b)Type-II H-shape power divider.

divider to facilitate laying out. The transition from the hollow waveguide to single-ridge is also shown in Fig. 3(b).

The H-shape power dividers of Type-I and Type-II should exhibit equal-amplitude and in-phase responses in a wide frequency band. For Type-I, the one-step transformer in each T-junction and steps #1 and #2 in the transition structure are combined to achieve impedance matching. By adjusting the length of one-step transformer M_x and height of step #1 H_1 (height of step #2 is fixed to be 2 mm), the reflection coefficient of Type-I divider can be improved, as shown in Fig. 4(a). A good reflection coefficient can be achieved when M_x= 0.3mm, H_1= 2.5 mm. For Type-II, two-step transformers are loaded in each T-junctions of the H-shape power divider to enhance the impedance matching bandwidth (See Fig.3(c)). Fig. 4(b) shows the simulated amplitude of Type-II divider with different values of *P*. It can be seen that the reflection coefficient is lower than -18 dB over the frequency range of 70-90 GHz when *P* = 2.1 mm. Fig. 5 shows the amplitude and phase responses of the two H-shape power dividers. Other dimensions of the feed network are given in Fig. 3. The output signal shows equal amplitude characteristics over the frequency range of 70-90 GHz. In the same frequency range, the output signals are in-phase between ports 3 (2) and 4 (5) but out-of-phase between ports 2 (4) and 3 (5). Considering the material and surface roughness and according to simulation, the loss of the whole feed network varies from 0.75 dB to 0.95 dB over the entire E-band.

III. Experimental Results

Two blocks, one for the radiation part (M1) and the other for the feed network (M2) are fabricated by milling with fabrication tolerance of 20 μm. Plenty of tightening screws are used to assemble the prototype and suppress the potential leakage between the two metal blocks. The photographs of fabricated blocks, assembled antenna and test environment are shown in Fig. 6. The overall size of the array antenna is 113 × 113 × 6 mm^3. The V- and W- band far-field antenna test systems with test accuracy of 0.5 dB are employed to test the radiation

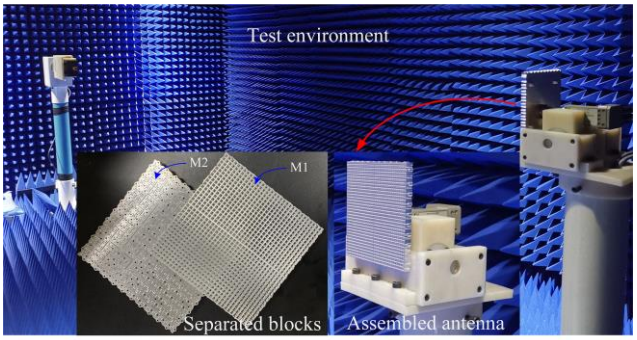

Fig. 6. Photographs of fabricated prototypes and test environment.

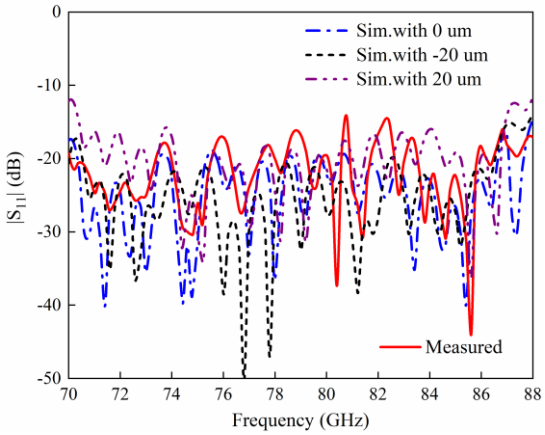

Fig. 7. Simulated and the measured reflection coefficients.

performances in a microwave chamber.

Fig. 7 compares the simulated and the measured reflection coefficients of the proposed array antenna. The measured results are slightly higher than the simulation results, but the overall trend remains consistent. Within the frequency range of 71–86 GHz (FBW: 19%), the measured reflection coefficient is below -13 dB. The difference mainly comes from the assembling errors and fabrication tolerance. The influence of fabrication tolerances on refection coefficient is roughly estimated and shown in Fig. 7. It shows the potential contribution of the fabrication tolerance to the discrepancy.

Fig. 8 shows the normalized radiation patterns in E- and H-planes at 71, 78.5, and 86 GHz. Simulation and measurement results are in good agreement, especially for the main lobes. The small differences can be attributed to measurement accuracy, imperfect assembly and fabrication. Over the entire frequency band, the measured 3-dB beamwidths and SLLs are less than 0.8° and 13 dB in both E-and H-planes. The measured cross-polarization radiation patterns are also plotted in Fig. 8. It shows a high cross-polarizations discrimination of over 34 dB for both planes over the same operating frequency band.

The simulated and measured peak gain and antenna efficiency are shown in Fig. 9, which exhibits a good agreement. The measured peak gain varies between 38.4 and 40.1 dBi from 71-86 GHz, and the simulated peak gain is approximately 0.1 to 0.5 dB higher than the measured value. This difference may be caused by the measurement and assembly inaccuracy, as well as the fabrication tolerance. The marginally larger difference in the low frequency range (71-75 GHz) is because this frequency range is close to the upper

frequency limit of the V-band test system and the test error may increase. A stable and high antenna efficiency of higher than 76.4% is obtained over 71-86 GHz. Table I compares this design with some previous published work based on hollow slotted waveguide. Different manufacturing processes, such as milling and diffusion bonding, are used to fabricate the prototypes. However, due to the restriction from the antenna structures, all previous designs required at least three blocks for fabrication and assembling. With the improved new feed network, the proposed array in this work can be realized with only two functional blocks. The antenna also exhibits a wide impedance bandwidth and high antenna efficiency.

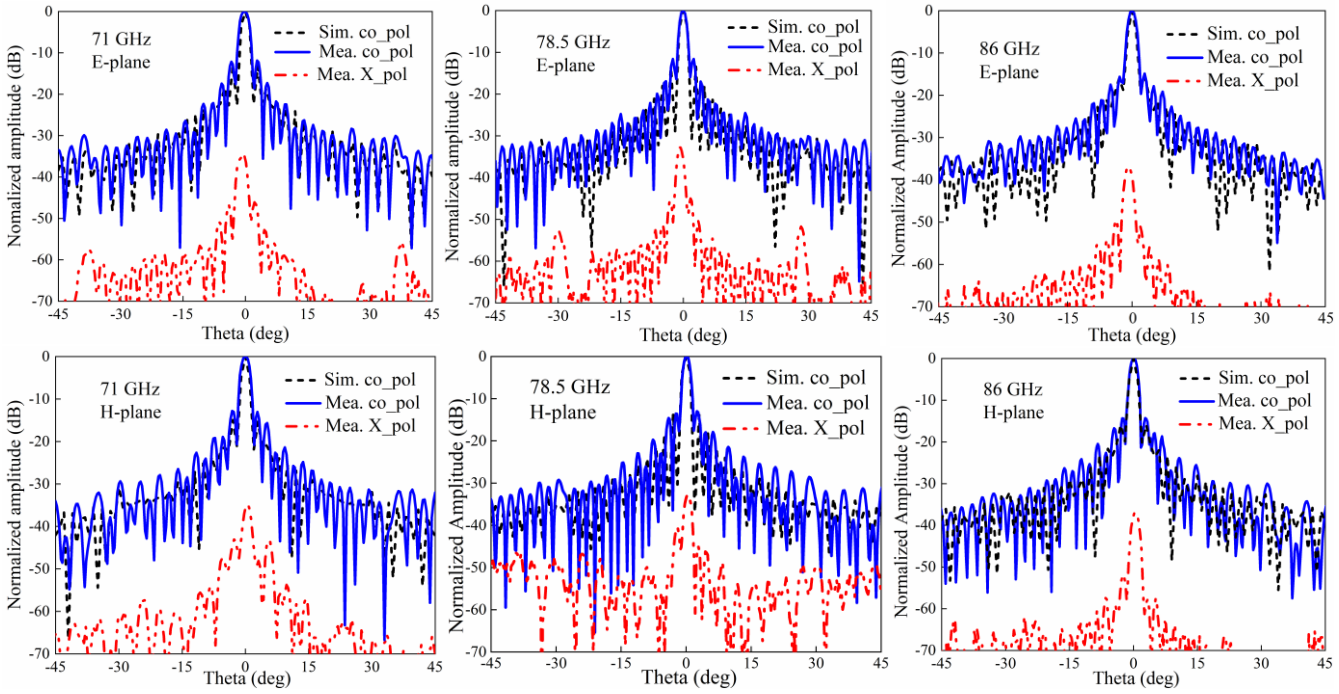

Fig. 8. Simulated and measured normalized radiation patterns.

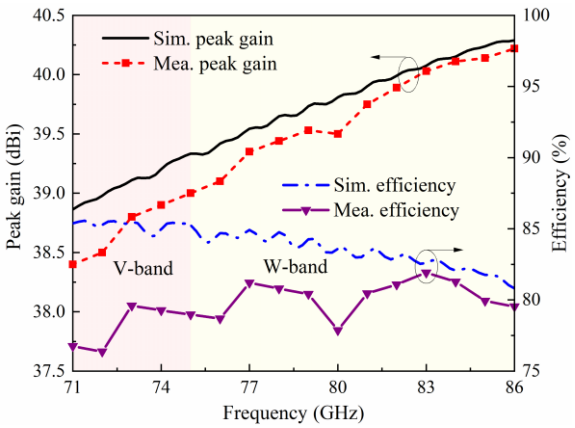

Fig. 9. Simulated and measured peak gain and efficiency.

IV. Conclusion

In this letter, we proposed an E-band full corporate-feed 32 × 32-slot array antenna implemented using only two circuit blocks. With the new feed network configuration, the cavity-backed layer in the conventional design was eliminated. This significantly reduces the antenna assembly, and therefore the manufacture cost, complexity, and the risk of electromagnetic energy leakage due to imperfect contacts between metal blocks. A prototype shows that the array antenna has an impedance bandwidth of over 19% and antenna efficiency of more than 76.4% over the whole E-band. This demonstration shows a good potential for mmW applications.

TABLE I
COMPARISON WITH SOME PREVIOUS WORKS

Ref.	Antenna type	FB(GHz)/ FBW	Blocks	AE	Peak gain (dBi)	Manufacturing process
[9]	16 × 16 slots	57-66/16%	3	70%	32.5	die-sink electric discharge machining
[11]	8 × 8 slots	28.3-35.3/22%	3	70%	23.5	die-sink electric discharge machining
[20]	32 × 32 slots	119-134/12%	>7*	60%	38	diffuse bonding
[21]	4 × 4 slots	118-140/17.6%	>10*	70%	21.1	diffuse bonding
This work	32 × 32 slots	71-86/19%	2	>76.4%	>38.4	milling

FB: Frequency band, AE: Antenna efficiency.
*Number of thin metal plates. At least three blocks are needed for fabrication if other manufacturing process is used.

REFERENCES

[1] Y. Yu, W. Hong, Z. H. Jiang, and H. Zhang, "E-band low-profile, wideband 45° linearly polarized slot-loaded patch and its array for millimeter-wave communications," *IEEE Trans. Antennas Propag.*, vol. 66, no. 8, pp. 4364–4369, Aug. 2018.

[2] E. Levine, G. Malamud, S. Shtrikman, and D. Treves, "A study of microstrip array antennas with the feed network," *IEEE Trans. Antennas Propag.*, vol. 37, no. 4, pp. 426–434, Apr. 1989.

[3] R. Chopra and G. Kumar, "Series- and corner-fed planar microstrip antenna arrays," *IEEE Trans. Antennas Propag.*, vol. 67, no. 9, pp. 5982-5990, Sep. 2019.

[4] X. Shen, Y. Liu, L. Zhao, G. Huang, X. Shi and Q. Huang, "A miniaturized microstrip antenna array at 5G millimeter-wave band," *IEEE Antennas Wireless Propag. Lett.*, vol. 18, no. 8, pp. 1671-1675, Aug. 2019.

[5] Wei Wang, Shun-Shi Zhong, Yu-Mei Zhang and Xian-Ling Liang, "A broadband slotted ridge waveguide antenna array," *IEEE Trans. Antennas Propag.*, vol. 54, no. 8, pp. 2416-2420, Aug. 2006.

[6] D. Kim and J. Lee, "Compact resonant slot array antenna using partial H-plane waveguide," *IEEE Antennas Wireless Propag. Lett.*, vol. 9, pp. 530-533, 2010.

[7] T. Li, H. Meng and W. Dou, "Design and implementation of dual-frequency dual-polarization slotted waveguide antenna array for Ka-band application," *IEEE Antennas Wireless Propag. Lett.*, vol. 13, pp. 1317-1320, 2014.

[8] L. Shi, C. Bencivenni, R. Maaskant, J. Wettergren, J. Pragt and M. Ivashina, "High-efficiency and wideband aperiodic array of uniformly excited slotted waveguide antennas designed through compressive sensing," *IEEE Trans. Antennas Propag.*, vol. 67, no. 5, pp. 2992-2999, May 2019.

[9] D. Zarifi, A. Farahbakhsh, A. U. Zaman and P. Kildal, "Design and fabrication of a high-gain 60-GHz corrugated slot antenna array with ridge gap waveguide distribution layer," *IEEE Trans. Antennas Propag.*, vol. 64, no. 7, pp. 2905-2913, July 2016.

[10] A. Farahbakhsh, D. Zarifi and A. U. Zaman, "A mm-wave wideband slot array antenna based on ridge gap waveguide with 30% bandwidth," *IEEE Trans. Antennas Propag.*, vol. 66, no. 2, pp. 1008-1013, Feb. 2018.

[11] M. Akbari, A. Farahbakhsh and A. Sebak, "Ridge gap waveguide multilevel sequential feeding network for high-gain circularly polarized array antenna," *IEEE Trans. Antennas Propag.*, vol. 67, no. 1, pp. 251-259, Jan. 2019.

[12] L. Chang, Z. Zhang, Y. Li and M. F. Iskander, "Air substrate slot array based on channelized coplanar waveguide," *IEEE Antennas Wireless Propag. Lett.*, vol. 16, pp. 892-895, 2017.

[13] F. Bauer and W. Menzel, "A 79-GHz resonant laminated waveguide slotted array antenna using novel shaped slots in LTCC," *IEEE Antennas Wireless Propag. Lett.*, vol. 12, pp. 296-299, 2013.

[14] Y. Tsunemitsu, S. Matsumoto, Y. Kazama, J. Hirokawa and M. Ando, "Reduction of aperture blockage in the center-feed alternating-phase fed single-layer slotted waveguide array antenna by E- to H-plane cross-junction power dividers," *IEEE Trans. Antennas Propag.*, vol. 56, no. 6, pp. 1787-1790, June 2008.

[15] A. Vosoogh and P. Kildal, "Corporate-fed planar 60-GHz slot array made of three unconnected metal layers using AMC pin surface for the gap waveguide," *IEEE Antennas Wireless Propag. Lett.*, vol. 15, pp. 1935-1938, 2016.

[16] S. Shad and H. Mehrpouyan, "60 GHz waveguide-fed cavity array antenna by multi-stepped slot aperture," *IEEE Antennas Wireless Propag. Lett.*, vol. 19, no. 3, pp. 438-442, March 2020.

[17] A. Vosoogh, A. Haddadi, A. U. Zaman, J. Yang, H. Zirath and A. A. Kishk, "*W* -band low-profile monopulse slot array antenna based on gap waveguide corporate-feed network," *IEEE Trans. Antennas Propag.*, vol. 66, no. 12, pp. 6997-7009, Dec. 2018.

[18] P. Liu, J. Liu,W. Hu, and X. Chen, "Hollow waveguide 32 × 32-slotarray antenna covering 71–86 GHz band by the technology of a polyetherimide fabrication," *IEEE Antennas Wireless Propag. Lett.*, vol. 17, no. 9, pp. 1635–1638, Sep. 2018.

[19] Y. Miura, J. Hirokawa, M. Ando, Y. Shibuya, and G. Yoshida, "Double-layer full-corporate-feed hollow-waveguide slot array antenna in the 60 GHz band," *IEEE Trans. Antennas Propag.*, vol. 59, no. 8, pp. 2844–2851, Aug. 2011.

[20] D. Kim, J. Hirokawa, M. Ando, J. Takeuchi, and A. Hirata, "64 × 64-element and 32×32-element slot array antennas using double-layer hollow waveguide corporate-feed in the 120 GHz band," *IEEE Trans. Antennas Propag.*, vol. 62, no. 3, pp. 1507–1512, Mar. 2014.

[21] D. Kim, J. Hirokawa, M. Ando, J. Takeuchi and A. Hirata, "4 × 4-element corporate-feed waveguide slot array antenna with cavities for the 120 GHz-band," *IEEE Trans. Antennas Propag.*, vol. 61, no. 12, pp. 5968-5975, Dec. 2013.